2012 IEEE International Conference on Robotics and Automation
RiverCentre, Saint Paul, Minnesota, USA
May 14-18, 2012

Conical Sidewinding

Chaohui Gong, Ross L. Hatton and Howie Choset

***Abstract*— Sidewinding is an efficient translation gait used by snakes and snake robots over flat ground, and resembles a helical tread moving over a core cylindrical geometry. Most sidewinding research has focused on straight-line translation of the snake, and less on steering capabilities. Here, we offer a new, geometrically intuitive method for steering this gait: Tapering the core cylinder into a cone, such that one end moves faster than the other, changing the heading of the robot as it drives forward. We present several design tools for working with this cone, along with experimental results on a physical robot turning at different rates.**

I. Introduction

Sidewinding is an efficient gait widely adopted by biological snakes and snake robots. During sidewinding, a snake makes static contact with part of the ground, as depicted in Fig 1, while keeping the rest of the body raised. By continuously passing the contacting segments along the length of its body, the snake is able to rapidly and efficiently transport itself through the world while incurring minimal frictional resistance from its environment. Sidewinding is especially useful on rocky, loose or slippery terrain, where the ground may not be strong or stable enough to provide the reaction forces necessary for other locomotion modes, such as lateral undulation [1] or other classes of "slithering." This friction minimization is also highly desirable for field-capable snake robots, which generally do not have the directional-friction properties that make slithering efficient in biological snakes.

The general working mechanism of sidewinding in terms of lifting and lowering actions was first revealed by Mosauer [2], and then given mathematical form by Burdick, Radford and Chirikjian [3]. In [4], we presented a simplified geometric model of sidewinding that interprets the lifting and lowering aspects of sidewinding as the rolling contact of helical tread revolving around a core geometry. This model, which implicitly made use of a *virtual chassis* [5] representation of the snake, allowed us to consider sidewinding as a simple "driving forward" action, leading us to wonder if there was a simple geometric model for steering sidewinding, such that we could control the motion in a fully car-like manner.

In general, changes in heading while sidewinding have received far less attention than their linear counterparts. Burdick *et al.* [3] noted that curving the "tracks" the sidewinder lays its body along will induce rotation, but also found that this operation significantly complicated their inverse kinematics approach, while in [6], we noted that sidewinding "forwards" and "backwards" with different halves of the snake would spin it in place, but did not further analyze this aspect. Re-examining our tread model, however, suggested an interesting geometric characteristic: tapering the tread along its axis (forming a cone) makes the robot roll in an orbit, rather than a straight line, and the curvature of its path can be controlled by adjusting the aperture of the cone.

Chaohui Gong is with the Department of Mechanical Engineering and the Robotics Institute, Carnegie Mellon University, chaohuig@cmu.edu

Ross L. Hatton and Howie Choset are with the Robotics Institute, Carnegie Mellon University, 5000 Forbes Ave., Pittsburgh, PA, USA rlhatton@cmu.edu & choset@cmu.edu

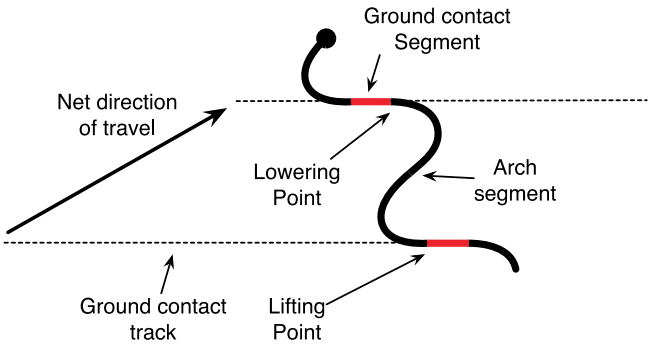

Fig. 1: Sidewinding motion. The ground contact segments are in static contact with the environment, while the arch segments are lifted from the ground and experience no friction. By progressively lifting the ground contact segments into arch segments while lowering arch segments down into ground contact segments, the snake or snake robot translates its body mass in the direction shown.

In this paper, we first review the principles of the tread model for sidewinding, and their extension to conical shapes. We then relate the geometric properties of a conical tread to the sidewinding paths it produces, and address lateral stability concerns that did not appear for the basic sidewinding gait. Finally, we verify the effectiveness and accuracy of our model through experimental tests on a physical snake robot.

II. Background

The results in this paper build on prior research into the motion of snakes and snake robots. While many approaches have been proposed to address the kinematics of snake-like systems, the three main developments that most contribute to the present work are continuous backbone curve representations, kinematic descriptions of sidewinding gaits and a reduced sidewinding model.

A. Backbone Curves

A powerful abstraction when working with snake robots is to step back from the specific characteristics of the robots and to work instead with a continuous *backbone curve* [7] describing the shape of the system. Doing so both simplifies the system representation, allowing access to the underlying physics of serpenoid motion, and makes the results of the analysis easily generalizable to snake robots with different actuation. Once the system motions have been worked out, a

978-1-4673-1404-6/12/$31.00 ©2012 IEEE

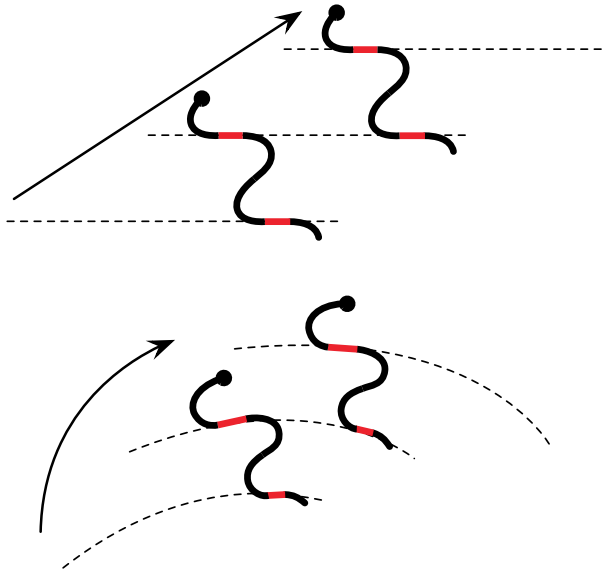

Fig. 2: With parallel ground contract tracks (top), the snake sidewinds in a straight line. If the tracks are curved (bottom), the snake sidewinds along an arc.

fitting algorithm, such as those of Chirikjian and Burdick [7] and Andersson [8] for planar and universal-joint designs, our formulation in [4] for alternating single-degree-of-freedom modules, or Yamada and Hirose's technique for arc-shaped joints [9] can be applied to map the backbone curve into the specific joint angle commands needed to implement the motion.

B. Sidewinding

Sidewinding is an efficient translation gait that is especially effective when crossing loose or slippery ground. While Mosauer [2] recognized the general mechanism of sidewinding, Burdick *et al.* [3] took the first effort to describe sidewinding in a rigorous mathematical fashion. Their analysis characterized the backbone shape during sidewinding as consisting of *ground contact segments* and *arch segments*. The ground contact segments are parallel to each other and in static contact with the environment. The "S"-shaped arch segments connect the ground contact segments, lifted from the ground lead to the movement relative to the environment. As illustrated in Fig. 1, the snake progressively raises one end of each ground contact segment into an arch segment, and lays down the arch segments into the other ends of the ground contacts. In doing so, the snake transfers its body mass between the *ground contact tracks* (GCTs), producing a net displacement.

In general, sidewinding is performed in straight-line paths over open ground, and produces a staggered sequence of straight GCTs, as shown at the top of Fig. 2. Burdick *et al.* [3] noted that sidewinding can be steered by curving the GCTs, as depicted at the bottom of the figure, and suggested that this motion could be implemented by laying down a desired trajectory of GCTs, then performing inverse kinematics to generate the corresponding sidewinding pattern.

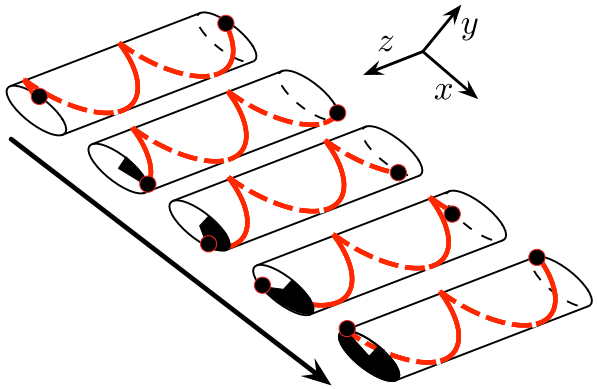

Fig. 3: The sidewinding backbone curve in our reduced model is an elliptical helix. As the backbone deforms over time, it acts as a helical tread around a hypothetical core cylinder, driving it forward.

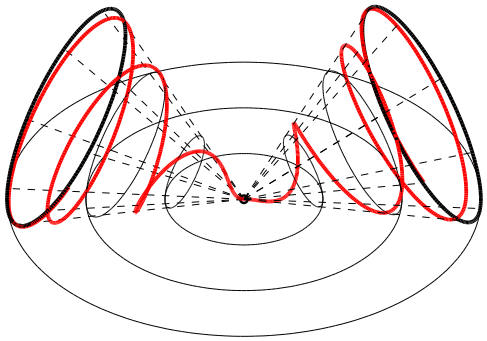

Fig. 4: The turning motion results from the virtual cone's rolling on the ground

C. Reduced Model of Sidewinding

In [10] we proposed a reduced model of sidewinding that interprets the motion from an external viewpoint. The roots of this reduced model can be found in Mosauer's [2] comparison of sidewinding to the motion of a rolling wire spring, and in Gray's [11] observation that sidewinding resembles the tread-drive of a tank or tractor. In our reduced model, we made these analogies concrete in a "virtual tread" model that takes the motion as a helical tread moving around a core elliptical cylinder. During sidewinding, the moving tread maintains rolling against the ground, driving the hypothetical cylinder forward, as illustrated in Fig. 3. This analytical model ignores the inner shape changes while focusing on the external geometric property, and as a result, simplifies associated motion analyses.

III. Analytical Model

Inspired by the observation that a cone rotates around its vertex as it rolls along flat ground, we have developed a steering approach to sidewinding that forms the snake robot into a similar conical shape. Consistent with our reduced model of sidewinding [10], the backbone curve of this gait is abstracted as a moving tread, but now on the surface of

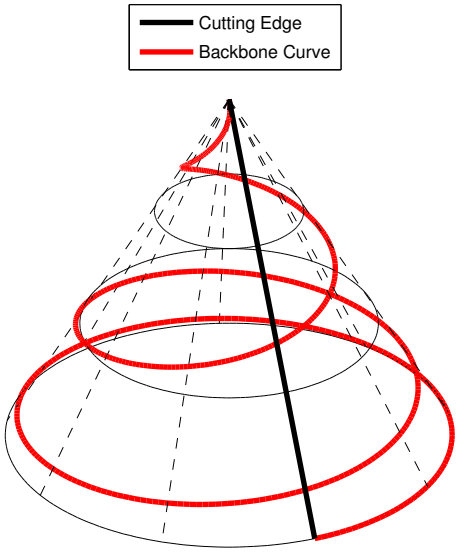

(a) Backbone curve on the surface of designed cone. The turning motion is determined by the taper of the inner cone.

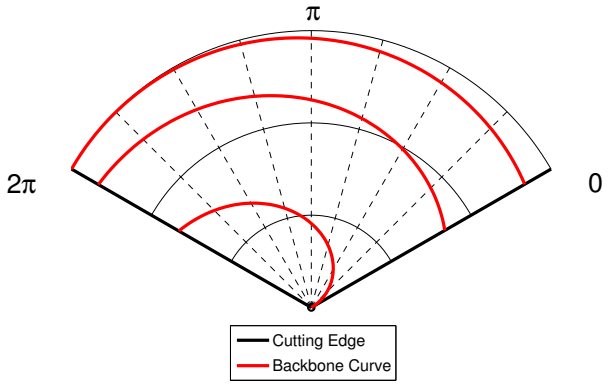

(b) Backbone curve on the sector by flatting the surface of the designed cone.

Fig. 5: Conical sidewinding's design is separated into two steps. First, according to desired turning rate choose the inner cone shape. Then, locate the backbone curve on the 2-d sector transformed from the cone surface.

a cone rather than a cylinder. This idea is similar to an observation made by Tanev in [12], while here we reveal an explicit relation between the shape of the core geometry and the motion generated. Fig. 4 demonstrates the geometric principles of conical sidewinding: as the cone rolls (or the tread moves around the cone), wider portions of the cone act as larger wheels and so translate faster than narrower portions, forcing the axis of the cone to rotate in the plane.

Because the backbone curve lies on the surface of a cone, the gait design naturally separates into two parts: choosing the shape of the cone, and then deciding how the backbone helix embeds into its surface. As discussed above, the taper of the cone determines the turning rate of the system, with an aperture angle of 2β making the cone rotate $\sin\beta$ in the plane for every radian it rolls. The second part is to identify the backbone curve's distribution on the cone's surface, which affects properties such as the lateral stability of the robot, as discussed in Section IV.

To simplify the backbone design, we reduce the three-dimensional backbone design problem to two dimensions by cutting the cone along one *generatrix* (straight line extending from the tip of the cone), as shown in Fig. 5(a), and unwrapping the cone into the solid arc section in Fig. 5(b). Cutting the cone, rather than projecting it into its base plane, offers the advantage of being a non-distorting transformation, thus preserving the mass-density of the backbone curve along its length.

Helical backbones on the cone may in general be described by taking r, the distance of a point on the backbone from the tip of the cone, as a function of the winding angle θ around the cone. In the unwrapped representation, these coordinates directly represent the radius of the backbone curve as a function of the polar angle, with the slight modification that each 2π range of θ is mapped to the arc-span of the unwrapped cone, rather than the full circle. In this paper, we specify the conical helix via a second-order curve of the form,

$$r(\theta) = a\theta^2 + b\theta + c, \tag{1}$$

balancing the richness and simplicity of the parameterization.

IV. Lateral Stability

In sidewinding, as in other forms of locomotion, it is important to ensure that the system remain stable and not overbalance. For sidewinding, pitch stability (in the direction of motion) is not a major concern, as the snake robot will inherently find a level resting configuration by rocking forward or backwards. Lateral stability, however, is a concern, especially for conical modes

When considering straight sidewinding's lateral stability, as long as there are integral number of loops on the cylinder surface, the stability is equivalent to a complete moving elliptical cylinder. Because of its even mass distribution along the central axis, the center of mass will always be located between two contact points. And as a result, when it is moving on the ground, it will not sway laterally. This assumption does not hold true, however, for conical sidewinding, because more mass will be distributed towards the base end of the cone, and because the tilt angle of the system may arrange the mass in an unstable orientation.

In three dimensions, this stability problem can be quite complicated. Even with the assumption that mass is evenly distributed along the backbone, the position of the center of mass must be calculated by averaging over all the points on the three-dimensional backbone curve. After that, position of the center of mass has to be projected onto the generatrix of the elliptical cone that is contacting the ground. Comparing this projection against the location of the ground contacts further requires that they themselves be calculated from the configuration of the cone.

Fortunately, our backbone design procedure simplifies the analysis by reducing the problem to two dimensions. As

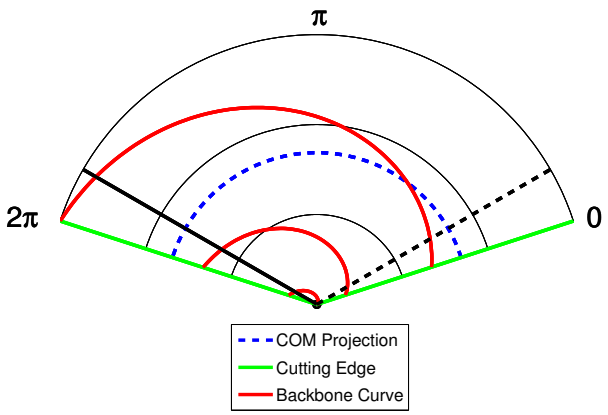

Fig. 6: This figure shows two different phases in the whole period of conical sidewinding. When the contacting points are located on the black solid generatrix, conical sidewinding is stable in roll direction. The dashed line indicates an unstable configuration.

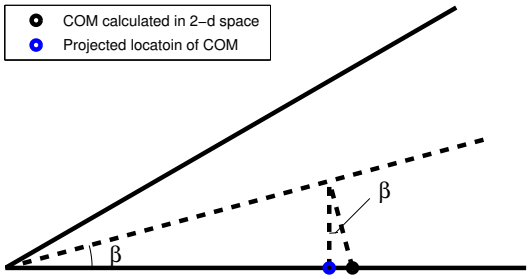

Fig. 7: The virtual cone's aperture is 2β, where β is the angle between the cone's lateral edge and its central axis. The black dot is the calculated location of the center of mass in our 2-d space, whose distance to the vertex equals to r_{COM}. The blue dot is the actual projected location from the center of mass onto the generatrix contacting the ground. β also defines the angle between the lines projecting from the central axis to these two points.

shown and Fig. 5(b), the backbone curve can be expressed as a function (such as that in (1)) of distance to the vertex and relative angle to a predefined generatrix. This function expresses the mass density as a function of θ, and the wrapping angle corresponding to the center of mass location can thus be calculated as

$$\theta_{\mathrm{COM}} = \frac{\int \theta \cdot r(\theta)\ \mathrm{d}\theta}{\int r(\theta)\ \mathrm{d}\theta}, \tag{2}$$

where θ maps the full wrapping from the head to the tail of the backbone curve around the cone. The corresponding radius of the center of mass can then be found by substituting θ_{com} into (1) and center of mass location can be found as

$$r_{\mathrm{COM}} = r(\theta_{\mathrm{COM}}). \tag{3}$$

Here, r_{COM} is the radius along the generatrix, and projects

Fig. 8: This is the snapshot of our snake robot moving on a predefined path using conical sidewinding gait. It is currently forming a cone shape, and turning around our desired center.

vertically as illustrated in Fig. 7: for a cone whose aperture is 2β, the distance from the cone's vertex to the projection of the center of mass can be expressed as

$$d_{COM} = \cos^2 \beta \cdot r_{COM}. \tag{4}$$

Finding the contact points is more straight forward. Suppose contacting generatrix's corresponding polar angle is θ_{g}, the contact points' locations can be directly solved as,

$$r_{\mathrm{contact}} = r(\theta_{\mathrm{g}} + C \cdot 2\pi) \tag{5}$$

where C is an integer ensures to find all the contact points inside the angle range.

Fig. 6 shows two phases within one whole period of conical sidewinding. The black lines represent the contacting generatrix, and the red line represents the backbone curve. The intersection between the black line and red line are the contact points and the blue dashed circle indicates the projection locus of the center of mass onto the contacting generatrix throughout the whole period. It can be observed that the black solid line corresponds to the moment the snake is in a stable configuration, while the black dashed line's corresponding configuration is unstable. When the ground contacting generatrix coincides to the black dashed line, the center of mass' projection is outside of the furtherest contacting point, making it an unstable configuration of roll stability.

V. Experiments

To demonstrate the effectiveness of controlling the snake's turning motion with our conical sidewinding model, we conducted several experiments. Each time, we fit the snake onto the surface of a virtual cone and commanded it to roll a complete circle on the ground. We recorded the tail positions during the experiment and compared them with the expected circles for the robot to follow. We fit best matching circles onto the recorded positions for each run, denoted as dashed circles in Fig. 9. The recorded trajectories for each gait closely match the corresponding circles, indicating

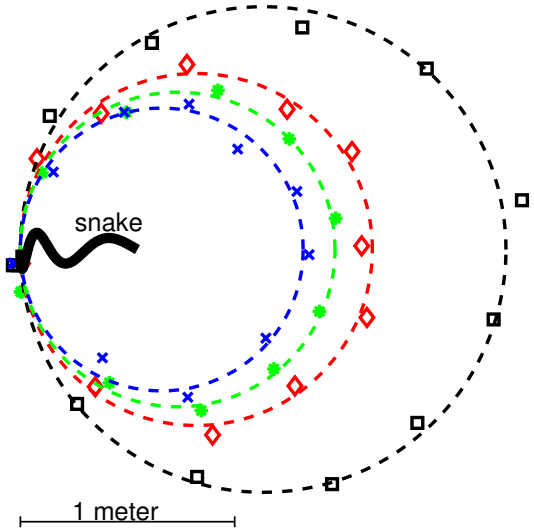

(a) Markers in this figure denote the recorded positions during our experiments. Different markers belong to different sets of experiments. The dashed circles are the best-fit circles to the measured data points. A snake is also drawn in this figure to show the scale.

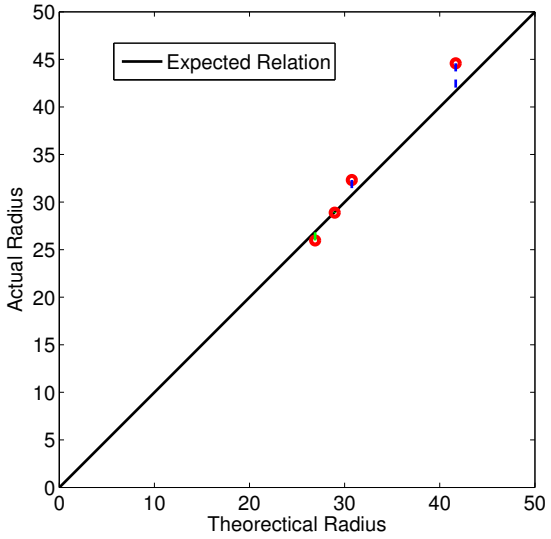

(b) The measured radiuses are very close to the theoretical calculations with maximum error of 6.55%. The black line is the 1:1 relation and circles are the sampled points. A perfect matching should locate on this straight line.

Fig. 9: Each time, we fit the snake robot to a virtual cone and let it roll a whole circle on the ground.

that the turning motion of conical sidewinding is near to a true cone's rolling on the ground, and that the turning motion is stable and consistent in each experiment. Fig. 9(b) provides a comparison between the measured turning radii and theoretical radii predicted from the conical apertures. The real turning radii turn out to be very close to our theoretical calculations based on cone's geometry, while we chiefly attribute the small deviations from the exact values to drag from the robot's tail.

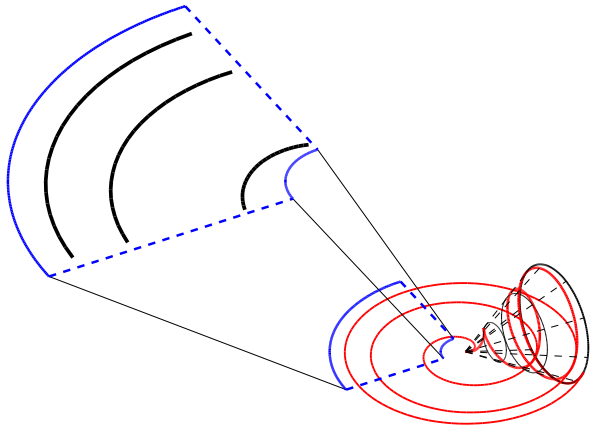

Fig. 10: The red curves show the ground contact tracks left on the ground by our conical sidewinding model. The black curves contained in the enlarged blue sector are part of the ground contact tracks.

VI. Conclusions and Future Work

Conical sidewinding provides new perspective from which to consider steering of this class of motion. As compared to previous efforts, the conical model offers a straight-forward geometric approach that can be intuitively controlled by changing the aperture of the cone. At the same time, our results match those of the earlier efforts, with the conical sidewinding producing the same curved ground contact tracks (illustrated in Fig. 10) as described in [3] and shown in Fig. 2

After the exploration of our mathematical model and accompanying experiments, we suggest several possible improvements on this reduced model. Throughout this work, the snake or snake robot is represented as a backbone curve along which mass is evenly distributed. However, because of the mechanical design and different material density, this reduced model is only a rough approximation. More powerful representation can be achieved by considering the true mass distribution along its body axis.

Additionally, initial results with our wave extraction method [13], suggest that conical sidewinding can be parameterized as a body wave of joint angles,

$$\alpha(n,t) = A(j) \cdot \sin\left(t - \phi(j)\right) \tag{6}$$

This parameterized equation can be used as a high level controller of sidewinding's turning motion. In other words, the turning rate will be directly controlled by changing these parameters online. After building the relation between these parameters to the geometric properties of the virtual cone shape, smooth transition from one shape to another shape can be realized by interpolating the parameters. This makes it possible for us to continuously change the snake's heading by choosing parameters corresponding to desired turning rate.

Acknowledgments

We would like to acknowledge the assistance of Matthew Tesch, Priya Deo, Andrew Burks and Ben Morse with the experimental portion of this work.

REFERENCES

[1] S. Hirose, *Biologically Inspired Robots (Snake-like Locomotor and Manipulator)*. Oxford University Press, 1993.

[2] W. Mosauer, "A Note on the Sidewinding Locomotion of Snakes," *The American Naturalist*, vol. 64, no. 691, pp. 179–183, March 1930.

[3] J. Burdick, J. Radford, and G. Chirikjian, "A "Sidewinding" Locomotion Gait for Hyper-redundant Robots," *Robotics and Automation*, vol. 3, pp. 101–106, 1993.

[4] R. L. Hatton and H. Choset, "Generating gaits for snake robots by annealed chain fitting and keyframe wave extraction," in *Proceedigns of the IEEE/RSJ International Conference on Intelligent Robots and Systems*, St. Louis, MO USA, October 2009.

[5] D. Rollinson and H. Choset, "Virtual chassis for snake robots," in *IEEE/RSJ International Conference on Intelligent Robots and Systems*, San Francisco, CA, USA, September 2011.

[6] M. Tesch, K. Lipkin, I. Brown, R. Hatton, A. Peck, J. Rembisz, and H. Choset, "Parameterized and scripted gaits for modular snake robots," *Advanced Robotics*, vol. 23, no. 9, pp. 1131–1158, 2009.

[7] G. Chirikjian and J. Burdick, "Kinematics of Hyper-redundant Locomotion with Applications to Grasping," in *International Conference on Robotics and Automation*, 1991.

[8] S. B. Andersson, "Discrete Approximations to Continuous Curves," in *IEEE International Conference on Robotics and Autmation*, 2006.

[9] T. Ohashi, H. Yamada, and S. Hirose, "Loop Forming Snake-like Robot ACM-R7 and Its Serpenoid Oval Control," in *Proceedings of the IEEE/RSJ International Conference on Intelligent Robots and Systems*, Taipei, Taiwan, October 2010.

[10] R. L. Hatton and H. Choset, "Sidewinding on slopes," in *Proceedings of the IEEE International Conference on Robotics and Automation*, Anchorage, AK USA, May 2010, pp. 691–696.

[11] J. Gray, "The Mechanism of Locomotion in Snakes," *Journal of Experimental Biology*, vol. 23, no. 2, pp. 101–123, December 1946.

[12] I. Tanev, T. Ray, and A. Buller, "Automated evolutionary design, robustness, and adaptation of sidewinding locomotion of a simulated snake-like robot," *Robotics, IEEE Transactions on*, vol. 21, no. 4, pp. 632 – 645, aug. 2005.

[13] R. L. Hatton and H. Choset, "Generating gaits for snake robots: Annealed chain fitting and keyframe wave extraction," *Autonomous Robots, Special Issue on Locomotion*, vol. 28, no. 3, April 2010.